

MedChemComm

Accepted Manuscript



This is an *Accepted Manuscript*, which has been through the Royal Society of Chemistry peer review process and has been accepted for publication.

Accepted Manuscripts are published online shortly after acceptance, before technical editing, formatting and proof reading. Using this free service, authors can make their results available to the community, in citable form, before we publish the edited article. We will replace this *Accepted Manuscript* with the edited and formatted *Advance Article* as soon as it is available.

You can find more information about *Accepted Manuscripts* in the [Information for Authors](#).

Please note that technical editing may introduce minor changes to the text and/or graphics, which may alter content. The journal's standard [Terms & Conditions](#) and the [Ethical guidelines](#) still apply. In no event shall the Royal Society of Chemistry be held responsible for any errors or omissions in this *Accepted Manuscript* or any consequences arising from the use of any information it contains.



Journal Name

ARTICLE

Injectable peptide hydrogels for controlled-release of opioids

Charlotte Martin,^a Edith Oyen,^a Jeroen Mangelschots,^a Mathieu Bibian,^a Tanila Ben Haddou,^b Jessica Andrade,^c James Gardiner,^c Bruno Van Mele,^d Annemieke Madder,^e Richard Hoogenboom,^f Mariana Spetea^b and Steven Ballet^{a*}

Received 00th January 20xx,
Accepted 00th January 20xx

DOI: 10.1039/x0xx00000x

www.rsc.org/

Herein, a family of hydrogel-forming peptides was designed starting from the short, tunable and amphipathic hexapeptide hydrogelator H-Phe-Glu-Phe-Gln-Phe-Lys-OH **1**. The hydrophobic side chains as well as the nature of both *N*- and *C*-termini were modified in order to obtain suited gelation conditions and drug release profiles for *in vivo* application. To potentially increase the enzymatic stability, an all-D analogue was prepared as well. After their macroscopic and microscopic characterization by rheology and transmission electron microscopy (TEM) analysis, opioid drugs were encapsulated into the hydrogels and sustained release experiments were carried out. Hydrogel toxicity was assessed in cell viability assays. Based on the physicochemical, mechanical, and nontoxic properties, H-Phe-Glu-Phe-Gln-Phe-Lys-NH₂ **2** was further investigated for *in vivo* release of morphine. The antinociceptive effects following subcutaneous injection of the morphine containing hydrogel **2** was evaluated in a model of thermal nociception using the mouse tail-flick test. Sustained antinociceptive effects over extended periods of time (up to 24 h) for morphine co-formulated with hydrogel **2**, compared to morphine injection in solution (effect up to 2h), were observed.

1. Introduction

Chronic pain remains a major societal burden that is associated with a decline of normal daily functioning and quality of life. For the treatment of moderate to severe chronic pain, around 90% of patients are treated with opioid analgesics.¹ Although opioid pain management causes severe side effects including respiratory depression, constipation, sedation, nausea, vomiting, development of analgesic tolerance, physical dependence and addiction potential, opioid analgesics still represent the most effective medication for the treatment of pain patients who have not responded to any other therapy.² To provide a good chronic pain relief, opioids can be administered using short-acting or long-acting formulations.³ In the case of short-acting opioid prescriptions, high doses are needed to reach the desired therapeutic effect,

due to the rapid and systemic biodegradation of the drug prior to interaction with the biological target. As a consequence, to provide consistent analgesia, opioid administration requires large and frequent doses to maintain effective plasmatic drug levels, resulting in the occurrence of common opioid-induced adverse effects. In contrast, long-acting opioid formulations improve quality of life of pain patients due to the slow release of analgesics and a longer duration of action.⁴⁻⁶ Extended release formulations were designed to enable a consistent and prolonged plasma drug concentrations within the therapeutic window, while reducing the risk of side effects and toxicity.⁷ To achieve sustained pain relief, it is necessary to develop proper drug delivery systems which can maintain a constant therapeutic effect without fluctuations in the physiological response.⁸ Around-the-clock analgesia can be realized using specific formulations for each administration route.⁹ Although oral medication prescriptions appear to be the first choice (i.e. easiest and least invasive administration mode), the limited duration of action due to first-pass metabolism of the drug represents a drawback for long treatments.¹⁰⁻¹¹ Additionally subcutaneous (s.c.)¹² and transdermal¹³ administrations are considered, but the need for implants¹⁴ and the lipophilicity¹⁵⁻¹⁶ of the drug represent limitations of these alternatives in pain research. Hence, versatile and biodegradable formulations that are compatible with a broad scope of physicochemical drug properties are of interest.

In this context, hydrogels have been reported as suitable controlled drug-delivery systems for compounds ranging from small molecules to biologicals.¹⁷ They are molecular networks

^a Research Group of Organic Chemistry, Vrije Universiteit Brussel, Pleinlaan 2, Brussels, B-1050, Belgium

^b Department of Pharmaceutical Chemistry, Institute of Pharmacy and Center for Molecular Biosciences (CMBI), University of Innsbruck, Innrain 80-82, A-6020 Innsbruck, Austria

^c CSIRO Materials Science & Engineering, Bayview Ave, Clayton, VIC 3169, Australia

^d Vrije Universiteit Brussel, Physical Chemistry and Polymer Science, Pleinlaan 2, B-1050 Brussels, Belgium

^e Organic and Biomimetic Chemistry Research Group, Ghent University, Krijgslaan 281, 9000 Ghent, Belgium

^f Supramolecular Chemistry Group, Ghent University, Krijgslaan 281, 9000 Ghent, Belgium

† Footnotes relating to the title and/or authors should appear here.

Electronic Supplementary Information (ESI) available: [details of any supplementary information available should be included here]. See DOI: 10.1039/x0xx00000x

that are capable of capturing an active ingredient while enclosing a large amount of water.¹⁸ Different types of hydrogels exist depending on the nature of the building blocks, the mechanical and structural characteristics, or the nature of cross-linking (physical or chemical).¹⁹ Chemical hydrogels are based on covalently cross-linked polymers that afford strong and irreversible hydrogels. Physical hydrogels result from the association of the composing building blocks (hydrogelators) by non-covalent interactions, such as hydrophobic interactions, hydrogen-bonding, π - π stacking interactions and Van der Waals interactions. Thanks to their biocompatibility, low toxicity and their physically crosslinked properties, peptide-based hydrogels represent an important class of injectable hydrogels,²⁰ suitable to be used as matrices for controlled and slow drug release.²¹ Peptide hydrogels loaded with active ingredients can liquefy during injection (shear thinning or thixotropic behavior), followed by quick hydrogel reformation once injected. These systems present several advantages such as protection of the drug against enzymatic degradation by encapsulation in the hydrogel network, while maintaining the therapeutic plasma drug concentration over a long period via diffusion from the hydrogel or by degradation of the network. Consequently, lower dosage and frequency of administration are possible, leading to a potential improvement of drug efficacy and concomitant reduction of side effects liability.

The development of peptide-based low molecular weight gelators (LMWGs) (MW < 1000 Da), which self-assemble into supramolecular gel matrices, takes advantage of easy and scalable synthesis with a limited cost.²²⁻²³ Among this family of LMWGs, one can find amphipathic α -peptides that self-assemble into β -sheet fibrils by non-covalent interactions, forming stable hydrogels in aqueous environment.²⁴

In this study, new amphipathic hexapeptide hydrogels have been developed and used for encapsulation and sustained release of two golden standard opioid drugs morphine and naloxone, an opioid antagonist. In case of morphine co-formulated with a hydrogel, sustained antinociceptive effects over extended periods of time (up to 24 h) after s.c. injection in mice is demonstrated.

2. Results and discussion

2.1 Design and Synthesis

The design of new amphipathic α -peptide hydrogelators (Table 1) was based on fine-tuning the previously reported sequence H-Phe-Glu-Phe-Gln-Phe-Lys-OH **1** (MBG-1), which presented very promising results in terms of *in vitro* controlled release of model cargoes.²⁵

The self-assembly process of hydrogelating peptides is influenced by different parameters such as the side chain hydrophobicity, ionic charges and the secondary structure propensity of the sequence. Indeed, formation of the β -sheets that underpin hydrogelation occurs by hydrogen-bonding,

noncovalent ionic and hydrophobic interactions between the side chains of the amino acids. Due to the very low pH (< 4) of MBG-1 hydrogel, this hydrogelator is not suited for *in vivo* applications, as painful injections could emerge. To increase the hydrogel's pH, it was envisaged that the *N*- and *C*-terminal amino and carboxylic acid groups of the sequence could be replaced, respectively, by an acetyl and a carboxamide, while keeping similar gelation properties.

Table 1. Amphipathic α -peptide hydrogelators with hydrophobic amino acids in blue and hydrophilic amino acids in red. D-amino acids are shown in lower case letters.

	Sequences
1 (MBG-1)	H-Phe-Glu-Phe-Gln-Phe-Lys-OH
2	H-Phe-Glu-Phe-Gln-Phe-Lys-NH ₂
3	Ac-Phe-Glu-Phe-Gln-Phe-Lys-NH ₂
4	H-phe-glu-phe-gln-phe-lys-NH ₂
5	H-Ile-Glu-Ile-Gln-Ile-Lys-NH ₂
6	H-Leu-Glu-Leu-Gln-Leu-Lys-NH ₂
7	H-Val-Glu-Val-Gln-Val-Lys-NH ₂
8	H-Ala-Glu-Ala-Gln-Ala-Lys-NH ₂
9	H-Cha-Glu-Cha-Gln-Cha-Lys-NH ₂

Peptide **2** possesses the same amino acid sequence as MBG-1 (Figure 1, left), but the presence of an amide instead of an acid at the *C*-terminus increased the gel's pH from 3.49 to 4.02. The gelation of **2** occurs by addition of phosphate buffered saline (PBS 10 mM; pH 7.4) at a concentration of 24 mM (2 % w/v).

This indicates that the *C*-terminus can be altered without impeding hydrogel formation. In contrast, the addition of an acetyl group at the *N*-terminus, affording peptide **3**, led to macroscopic aggregation under the same gelation conditions (PBS 10 mM; pH 7.4). This indicates that in this type of sequences the charge of the amine is necessary for self-assembly and stabilization of fibrous structures. Based on the premise that the free amine at the *N*-terminus is needed, while the *C*-terminal amide is tolerated for peptide self-assembly, the importance of aromaticity at the hydrophobic side of the β -sheets was investigated next via replacement of Phe residues by aliphatic ones (peptides **5-9**, Table 1). As the driving force of hydrogelation is amphipathicity in this family of peptides, the size, hydrophobic character and aromaticity of the amino acid side chains were considered. Among all these sequences, only peptides **5** and **9** formed gels at 2% w/v

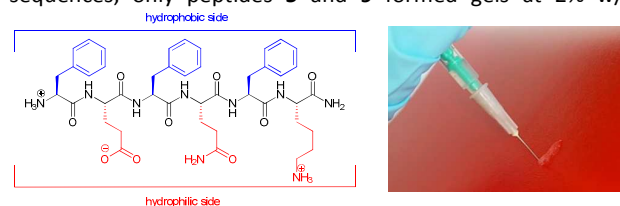


Figure 1. Structure of peptide hydrogelator **2** at pH 7.4 (left) and immediate re-gelation after injection through a 25G needle used for s.c. injections (right).

concentration in PBS, whereas analogues **6**, **7** and **8** remained in solution.

These results can be explained by the relative lipophilicity of the composing amino acids. Indeed, at pH 7 Phe is classified as the most hydrophobic residue, followed by Ile, Leu, Val and Ala.²⁶ The last sequence of this set, sequence **9**, was designed to investigate the influence of aromaticity on the hydrogelation process. Cyclohexylalanine (Cha) is an unnatural amino acid, which can be regarded as the saturated version of Phe, with a significantly higher hydrophobicity. Although replacement of Phe by Ile or Cha still allows formation of a hydrogel, the respective rheological data (vide infra and SI) showed the formation of weaker gels, as compared to **2** indicating that π - π stacking interactions are important for hydrogel formation.

The use of α -peptide hydrogelators, synthesized from natural amino acids, is extremely attractive for *in vivo* applications as such systems might easily be degraded by proteolytic enzymes, giving way to non-toxic amino acid and peptide segments. For application as drug delivery systems, peptide hydrogel systems can potentially also modulate release kinetics by alteration of the sequence. Control over drug-hydrogel fiber interactions and proteolytic degradation, could influence the release properties. To achieve prolonged *in vivo* stability, unnatural amino acids such as D-amino acids or β -amino acids can be used. The incorporation of D-amino acids, within amphipathic peptide hydrogelators, was reported beneficial for their biostability, but the most important challenge with such modifications consists in retaining the gelling behavior. Indeed it was also reported that the switch of chirality from L to D of only one amino acid can disturb the self-assembly of β -sheets, giving way to the loss of gel properties. Therefore, the synthesis of all-D sequence **4** was performed; wherein all L-amino acids were exchanged by the corresponding D-amino acids. Because hydrogelators **2** and **4** presented the most promising physicochemical and gelation properties, subsequent *in vitro* and *in vivo* studies focused on these two sequences.

2.2 Hydrogel characterization

The first step to characterize peptide hydrogels consists of applying the qualitative tilted tube method, in order to demonstrate the formation of a self-supporting gel. Both sequences **2** and **4** gave a transparent gel in the same conditions (PBS 10 mM at pH 7.4 with a minimum gelation concentration of 24 mM; 2% w/v). To evaluate the mechanical properties of these hydrogels in a more quantitative manner, rheological experiments were performed. The viscoelastic properties of the peptide hydrogels were measured by dynamic rheometry at 37 °C. This technique allows to measure the storage modulus G' (corresponding to the material's stiffness or rigidity), loss modulus G'' (corresponding to the viscous properties of the material) and loss factor $\tan(\delta)$ (ratio of G'' over G'). According to the Winter-Chambon criterion, a material reaches gelation in rheological terms if the phase

angle δ gets frequency-independent.²⁷⁻²⁸ However, the profiles of the peptide hydrogels showed a declining δ as a function of frequency, corresponding to 'structured fluids' or 'weak gels', according to rheology (see Supporting Information).²⁹

Peptide hydrogel **2** showed a G' value of ca. 8000 Pa (Figure S1, value taken at a frequency of 1 Hz), comparable to its precursor MBG-1, which was described as a rather rigid hydrogel.²⁵ Hydrogelator **4** (SI Figure S1) gave way to a less rigid hydrogel, having a G' value of ca. 1000 Pa.

In addition, transmission electron microscopy (TEM) was used to investigate the fiber morphology of the resulting hydrogels. For the hydrogels based on sequences **2** and **4**, long, entangled fibers were observed, forming the hydrogel network (SI Figure S2). Peptide hydrogel **2** forms fibrils having a clear twist, whereas all-D sequence **4** forms straight fibers. Both hydrogels contain fibers having a comparable thickness of ca. 10 nm.

2.3 *In vitro* stability

The stability (defined as half life, $t_{1/2}$) of the peptide hydrogels in human plasma at 37°C was investigated for sequences **2** and **4**. While the half-life of **2** was calculated to be around 15 min (SI Figure S3), the corresponding C-terminal carboxylic acid presented a half-life of approximately 2 min. Improved plasma stability is commonly observed for C-terminal carboxamides. However, no half-life could be determined for the sequence containing D-amino acids. As expected, after 4 days of incubation with human plasma, all-D-analogue **4** remained intact. The straightforward use of D-amino acids to synthesize stabilized peptide-based hydrogelator induces an exceptional increase of resistance towards proteolytic degradation.

2.4 *In vitro* release experiments

The ability of peptide hydrogels from **2** and **4** to release bioactive molecules was first studied via *in vitro* experiments. These consisted of a static drug release from the hydrogel within an Eppendorf, using PBS as a physiologically relevant medium. Even though these experiments are not equivalent to behavior in *in vivo* environments, especially because no proteases are present, they give an idea of the peptide's capacity to retain the investigated drugs. In the applied *in vitro* setting, the geometry of the sample, the aliquoting method, the volume of acceptor medium, and the hydrogel swelling/degradation/erosion properties will determine the release profile.

As morphine is the most commonly analgesic drug clinically used to date for chronic pain management,³⁰ it was chosen as an opioid agonist cargo to gain first insights into the release kinetics from the hydrogels described above. Additionally, a structurally related opioid antagonist, naloxone, was included in the study as well. The controlled release of mixed opioid agonist-antagonist systems (e.g. oxycodone-naloxone formulations) has been investigated for treatment of chronic low back pain, and hence this cargo molecule is also clinically relevant.³¹

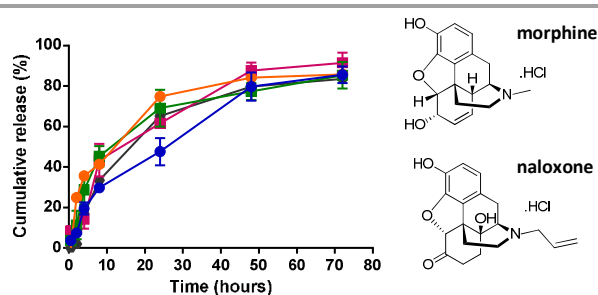


Figure 2. Release profiles of morphine hydrochloride (3.1 mM; 0.1% w/v) and naloxone hydrochloride (0.5 mM; 0.02% w/v) from the self-assembled peptide hydrogels **2** (2% w/v, in blue and orange, respectively) and **4** (2% w/v, in green and pink, respectively) and morphine hydrochloride (103 mM; 3.3% w/v) from hydrogelator **2** (2% w/v, in grey) in PBS (10 mM, pH 7.4) at room temperature using a static release model. Data points represent the average of 3 samples with calculated error bars.

Morphine was diluted in PBS to obtain a solution with a concentration of 3.1 mM (0.1% w/v). The resulting solution was directly added to the peptidic hydrogelator in an Eppendorf, to construct the drug delivery system loaded with morphine hydrochloride and ready for the release study. In this release model, hydrogels are gently covered with PBS. From this moment, the sampling of supernatant aliquots at regular time points starts, and the samples are replaced with fresh PBS to keep a constant volume. HPLC measurements at 215 nm were performed, allowing to plot the percentage of released morphine hydrochloride as a function of time based on a calibration curve (Figure 2). Overall, the morphine *in vitro* release profiles are characterized by a rapid initial release during the first hours (i.e. a burst effect), followed by a sustained release over 3 days resulting in a recovery of about 90%. Interestingly, an increase of the morphine concentration to 3.3% w/v does not influence the release profile. This small burst effect (approximately 20%) can be attributed to fast morphine diffusion through the large pores of the hydrogel, the release of molecules which are weakly associated to the network, and/or the rapid evasion of drug molecules present at the surface of the hydrogel. This phenomenon causes considerable release at the initial stage, but should not necessarily be considered as a drawback. In fact, a moderate burst effect may be useful to provide immediate pain relief, followed by a prolonged therapeutic effect.³²

Comparison between the 'native' sequence **2** and the more stable **4**, both at room temperature, shows almost identical release rate of morphine, which may have been anticipated as no proteases were present. The influence of temperature (physiological temperature 37°C) on the kinetic of morphine release was also investigated for both hydrogelators at 2% w/v concentration (data not shown). At physiological temperature, the same release profiles were obtained. These *in vitro* release

curves of morphine held promise for subsequent *in vivo* experiments.

2.5 Biological evaluation

Cytotoxicity

Optical microscopy images of L929 cells grown on 96 well plates coated with peptide hydrogels **2** and **4** for a period of 24 h, showed cells with a somewhat rounded morphology (see SI Figure S4), indicating that the cells did not spread on the peptide hydrogels, in contrast to the cells of the control TCPS plates (SI Figure S4-B). The cytotoxicity of the hydrogels was qualitatively assessed using the Live/Dead cell viability assay (Invitrogen, see SI Figure S4-C and S4-D) after 24 h of cell culturing on peptide hydrogels. For peptide hydrogel **2**; this assay showed that the majority of cells were green fluorescent and thus, were viable in a similar way to those cultivated on control ULA plates (see SI Figure S4-A). This peptide hydrogel can therefore be considered as biocompatible. Surprisingly, after 24 h hydrogel sequence **4** possessed an evenly distributed number of red and green fluorescent cells. The reason for the increased number of red fluorescent cells, as compared to hydrogels **2** is unclear, but this result is indicative of cytotoxicity and hence all-D sequence **4** was not considered for any further *in vivo* testing. Toxicity of all-D peptides has previously been described in literature.³³

Antinociceptive effect

Prior to the planned *in vivo* experiments, the injectability of the hydrogels was tested and confirmed by the use of a 25G needle destined for s.c. injections (see Figure 1 and movie in Supporting Information). The mechanical properties of hydrogels resulting from the co-formulation of morphine with hydrogelator **2** were also investigated (SI Figure S5). Upon loading 0.5 mg of morphine (0.3% w/v), a G' value comparable to the one of a hydrogel without cargo was obtained (ca. 2200 Pa). In contrast, higher morphine concentrations (5 mg and 10 mg, corresponding to 3.3 % and 6.6 % w/v) increase the gels' rigidity (G' of 3400 Pa and 6500 Pa, resp.). The increased stiffness of the hydrogels can be explained by hydrophobic interactions between morphine and the hydrogelator. Next, the *in vivo* efficiency of sequence **2** as a drug delivery platform was investigated through controlled release experiments of morphine.

Morphine's relatively short duration of analgesic action, renders it a suitable model to evaluate prolonged effects generated by co-formulation with hydrogel **2**. The therapeutic antinociceptive effect was investigated in a model of thermal nociception using the tail-flick test in mice (Figure 3). In this set of experiments, morphine was injected s.c. in solution or co-formulated with hydrogel **2**, following the same protocol as described above for the *in vitro* release study (i.e. using physiological saline solution). First, we selected a dose of morphine of 5 mg/kg, which produces an antinociceptive effect corresponding to 80% of Maximum Possible Effect (%MPE). As shown in Figure 3 (red curve), morphine

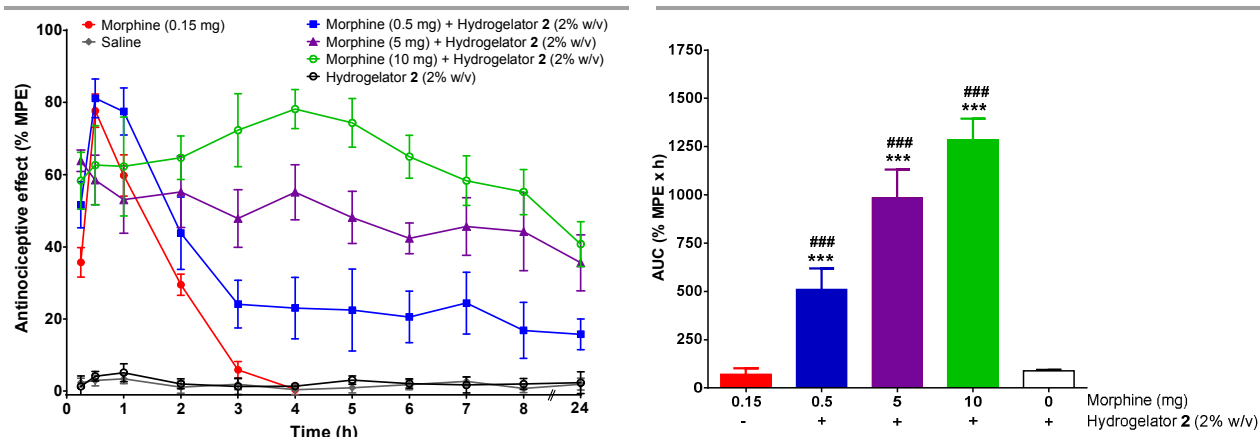


Figure 3. Antinociceptive effects of morphine in the mouse tail-flick test after s.c. administration, applied in solution or co-formulated with hydrogelator 2 (2% w/v). Left panel: Time course of the antinociceptive response as % of Maximum Possible Effect (%MPE). Right panel: Areas under the curves (AUC) of the respective time curves. Doses of morphine are given per mouse. Data are the mean \pm SEM of 5 to 10 mice per group. *** p < 0.001 vs. group treated with morphine in solution, ### p < 0.001 vs. control group treated only with hydrogelator 2 (2% w/v) (ANOVA with Tukey's post-hoc test).

administered s.c. in bolus at a dose of 5 mg/kg produces a marked antinociceptive response with a peak of action at 30 min which declined rapidly thereafter, with no effect detected at 3 h after drug administration. This dose of morphine, corresponding to a dose of 0.15 mg per mouse, served as a reference to compare the influence of hydrogelator 2 as a novel drug delivery system. Since higher doses are typically applied when sustained release devices are used compared to bolus injections, to reach prolonged therapeutic effects, the first tested dose per mouse consisted of a co-formulation including 0.5 mg of morphine and hydrogelator 2 at a concentration of 2% w/v (Figure 3, blue curve). This formulation led to a minor improvement of the maximal possible effect from 3 h post-injection onwards. An extended, but limited effect detectable up to 24 h was noticed (*ca.* 20% of MPE). These experiments indicate that a threefold increase of morphine dose did not suffice to extend the antinociceptive response. Hence, the dose of morphine in co-formulation with hydrogelator 2 (2% w/v) was increased. At both tested doses of 5 mg and 10 mg per mouse (Figure 3, purple and green curves, respectively) the desired extended release profiles were obtained, with an antinociceptive effect of *ca.* 40% MPE for the 10 mg dose, after 24 h.

Upon application of higher doses (5 and 10 mg/150 μ L) the peak antinociceptive effect was absent or much delayed. This observation can potentially be related to the increased gel stiffness, resulting from higher drug loadings (*vide supra*). One remarkable advantage of the current formulation is the large drug loading capacities that are possible (up to *ca.* 77%) with this type of peptide hydrogelator, yet keeping the injectable gel properties. Higher doses were not considered given the limited solubility of morphine. Notably, apart from a slight increase in motor activity, no sedative effects or other typical opioid side effects were observed in mice, even upon

application of the highest injected dose of morphine co-formulated with hydrogelator 2.

3. Conclusion

In summary, we developed a novel short amphipathic peptide-based hydrogel that forms a thixotropic injectable gel under physiologically relevant conditions. The hydrophobicity of the amino acid side chains in these amphipathic peptides was varied and showed that aromaticity of the Phe residues is key for the formation of rigid hydrogels, as aliphatic side chains resulted in no hydrogel formation or less rigid hydrogels. The most interesting sequence 2 and its all-D counterpart 4 were characterized by TEM revealing the formation of nanofibrillar networks which could be used for the entrapment and controlled release of drugs.

Once interesting *in vitro* drug release profiles of morphine and naloxone were observed in a static release model over 3 days, the noncytotoxic nature of the hydrogelator 2 was demonstrated while hydrogelator 4 was unexpectedly found to be cytotoxic. The beneficial role of the hydrogel formulations, in comparison with bolus injections in solution was clearly established via monitoring of morphine's antinociceptive effect in mice using the tail-flick test model after subcutaneous injection. The high drug loading capacity (up to *ca.* 77%) of the peptide-hydrogel system allowed to maintain a significant antinociceptive effect of around 40 % of MPE after 24 h, without major alterations in the general behavior of mice during treatment. The absence of adverse effects is indicative of the high stability of the hydrogel after s.c. injection. Because of the growing burden of chronic pain on the society, efficient and economically viable formulations used for prolonged pain treatment remain of high interest. The presented hydrogels could serve as a drug delivery platform, and can clearly be applied beyond the development of extended release formulations of analgesics.

4. Experimental section

4.1 Chemistry

Peptide synthesis: Peptides were synthesized according to the standard solid-phase peptide synthesis method.³⁴ Peptide purification was performed using preparative reverse high-performance liquid chromatography. A linear chromatography gradient starting from 10% of acetonitrile (+ 0.1% trifluoroacetic acid) to 80% in 20 min was used with a linear gradient. Trifluoroacetic acid (TFA) salt of pure product was obtained after lyophilisation of collected fractions.

Peptide gelation: The peptide gelation occurs by dissolving the TFA salt of the hexapeptide (2mg) in 100 μ L of PBS solution (pH 7.4).

4.2 Characterization

Rheology: Dynamic rheometry measurements were performed on an AR-G2 rheometer (TA Instruments) equipped with electrically heated plates and a 10 mm-diameter aluminium parallel plate-plate geometry. Viscoelastic properties were measured by oscillatory frequency sweeps at 37 °C in the range between 0.01 and 10 Hz, using a controlled strain of 0.05 %. Hydrogel samples were made 24 h in advance. A ring-shaped reservoir filled with a saturated NH_4Cl solution was used as a solvent trap.

TEM: Formvar carbon-coated 400-mesh copper grids (Agar Scientific, Stansted, United Kingdom) were treated with plasma using an ELMO Glow discharge system to clean the grid surface and to render the carbon surface hydrophilic. Hydrogel samples were prepared 24 h in advance as described above. Small aliquots of sample (5 μ L) were pipetted onto the carbon grids for adsorption. After 30 s, excess of sample was removed by using a Whatman 541 filter paper. The loaded grids were stained during 10 s with 1 % uranyl formate after which the grids were air-dried. Samples were analysed using a JEOL JEM-1400 transmission electron microscope, operating at accelerating voltage of 120 kV. Images were recorded on a CMOS TemCam-F416 camera and accessory software of TVIPS.

Cryo-TEM: 200-mesh copper grids coated with perforated carbon film (Lacey carbon film: ProSci-Tech Qld, Australia) were used and were glow discharged in nitrogen for 5 s immediately prior to use. Hydrogel samples were prepared 24 h in advance as described above. Small aliquots of sample (4 μ L) were pipetted onto the carbon grids for adsorption. After 30 s, excess of sample was removed by using a Whatman 541 filter paper. The grid was then plunged into liquid ethane cooled by liquid nitrogen. Frozen grids were stored in liquid nitrogen until required. Samples were analysed using a Gatan 626 cryoholder and Tecnai 12 Transmission electron microscope, operating at accelerating voltage of 120 kV. Images were recorded using an FEI Eagle 4k x 4k CCD camera.

4.3 *In vitro* stability

Human plasma was obtained from the Belgian Red Cross (Vlaams-Brabant, Leuven). Prior to the stability test, selectivity,

stability of the compound in the injection solvent, the effect of various incubation times at 4°C, linearity, accuracy and precision of the method were investigated. Frozen (-20°C) human plasma samples were thawed and thermostated to 37±2°C. Dissolution of the lyophilized peptide and consecutive dilutions were performed in water. The resulting aqueous solutions of peptides **2** and **4** were spiked in human plasma (10:90 v/v) with final plasma concentrations of 34, 33, 33 and 33 μ M, respectively. During the plasma stability study, samples were taken after 0, 5, 10, 15, 30, 60, 90, 120, 240, 1500 and 5700 min for peptide **4** and 0, 5, 10, 15, 30, 60, 90 and 120 min for peptide **2**. On every time point 100 μ L spiked plasma was transferred to a 500 μ L Eppendorf tube and a protein crash was performed using 300 μ L methanol + 0,1% TFA (4°C). Suspensions were vortexed for 15 seconds and placed at 4°C for 30 to 45 minutes. After centrifugation at 18 625 g for 20 minutes, 100 μ L supernatant was diluted with 100 μ L water in the injection vial. Injection samples were vortexed for 5 seconds and placed in the autosampler. For the calculation of the peptide half-life, only points with an area under the curve (AUC) higher than the AUC of the lowest standard were used. Concentrations were calculated by use of the calibration curve and transferred to a semi-log chart presenting the log concentrations as a function of time. The optimum curve was used to calculate the peptide-half life. Calculations were performed using Microsoft® Office Professional 2010 Excel.

4.3 *In vitro* release experiments

Loaded drug delivery system was prepared by addition of 100 μ L of PBS solution containing morphine hydrochloride with a concentration of 0.1% w/v on 2 mg peptide hydrogelator in an Eppendorf of 1.5 mL. PBS (0.5 mL) was gently added on the top of the resulting loaded hydrogel. This last step is the starting point for the kinetic monitoring. At selected time points, aliquots (10 μ L) of the supernatant PBS were taken and were replaced by fresh PBS. For each sample, UV spectra (using analytical HPLC) were recorded and the absorbance signal was integrated at 215 nm. The percentage release profile of morphine was obtained by plotting the percent fraction as a function of time. The experiments were repeated in triplicate, and allowed to calculate the error bars.

4.4 Biological evaluation

Cytotoxicity

Cell viability Assay: L929 (mouse fibroblast) cells were obtained from ATCC® and maintained in Gibco®, MEM with GlutaMAX supplemented with 10% FBS (SAFC, Sigma), 1% Anti-Anti (100X, Gibco®) and 1% NEAA (100X, Gibco®). Cells were maintained on tissue culture treated polystyrene (TCPS) plates at 37°C in a humidified atmosphere containing 5% CO_2 and 95% air. Cells were trypsinized, harvested and counted using a hemocytometer. The resulting cell suspension was diluted in Gibco® solution before addition to the hydrogels. For ease of handling and to produce homogeneous clear hydrogels, 100 μ L of peptide hydrogels were prepared (in corresponding gelation conditions, see above) in Eppendorf tubes (0.5 mL) and

transported using a 21G syringe to 96-well plates after simultaneously heating (60°C) and mixing (900 rpm) using an Eppendorf ThermoMixer®. The hydrogels were left to set overnight in the wells at room temperature and were subsequently washed twice with 200 µL of Anti-Anti (100X, Gibco®) solution, 2 h each. After washing, media was removed and cells were seeded evenly over hydrogels. Cells were plated in duplicate on all hydrogels and control wells. Viability of cells on hydrogels was determined using the traditional Live/dead cell viability assay (Invitrogen) after culture durations of 24 h.

Live/Dead Cell Viability Assay: Cells were plated in duplicate (1 x 10⁵ cell/well in 16 well plates) on control TCPS culture plate, control ULA plate and ULA plate containing the nanostructured hydrogels (including hydrogelator **2**, hydrogelator **4**). Plates were incubated in 5% CO₂ at 37°C for 1 day to allow cell attachment and spreading to occur. Live/dead cell viability assay was done using "LIVE/DEAD® Viability/Cytotoxicity Kit *for mammalian cells* (Invitrogen) as per the manufacturer's instructions. Details of the assay are provided in the Supporting Information.

Nociceptive assessment

Animals and drug administration: Male CD1 mice (6-8 weeks old, body weight average 30 g) were obtained from Charles River (Sulzfeld, Germany). Mice were group-housed in a temperature controlled room with a 12 h light/dark cycle and with free access to food and water. All animal studies were conducted in accordance with ethical guidelines and animal welfare standards according to Austrian regulations for animal research, and were approved by the Committee of Animal Care of the Austrian Federal Ministry of Science and Research. Groups of mice were s.c. administered either (1) morphine (Gatt-Koller GmbH, Innsbruck, Austria) dissolved in sterile physiological saline (0.9%) as bolus in a dose of 5 mg/kg (corresponding to 0.15 mg per mouse, volume of 10 µl/g body weight), (2) morphine (0.5, 5 or 10 mg per mouse, in a volume of 150 µl) formulated with hydrogelator **2** (2% w/v) in physiological saline or (3) saline or hydrogelator **2** (2% w/v) only used as controls. Each experimental group included five to ten animals.

Tail-flick test: The radiant heat tail-flick test was used to assess antinociceptive effects of tested drugs after s.c. administration in mice using an UB 37360 Ugo Basile analgesiometer (Ugo Basile s.r.l., Varese, Italy) as described previously.³⁵ The reaction time required by the mouse to remove its tail due to the radiant heat was measured and defined as the tail-flick latency. A cut-off time of 10 s was also used in order to minimize tissue damage. The antinociceptive response was expressed as percent of Maximum Possible Effect (%MPE) = [(TL - BL)/(cut-off time - BL)] x 100. Data were analyzed with ANOVA using Tukey's multiple comparison test, and graphically processed with the GraphPad Prism Software (GraphPad Software Inc., San Diego, CA).

Acknowledgements

We thank the Research Foundation–Flanders (FWO Vlaanderen) for the financial support. This work is also supported by the Scientific Research Network (WOG) "Supramolecular Chemistry and Materials" of the Research Foundation-Flanders and the Austrian Science Fund (FWF): TRP 19-B18. We gratefully acknowledge Yannick Van Wansele and Dr. Ann Van Eeckhaut for assistance with the *in vitro* stability tests.

Notes and references

1. A. M. Trescot, M. V. Boswell, S. L. Atluri, H. C. Hansen, T. R. Deer, S. Abdi, J. F. Jasper, V. Singh, A. E. Jordan and B. W. Johnson, *Pain Physician*, 2006, **9**, 1.
2. J. C. Ballantyne and N. S. Shin, *Clin. J. Pain*, 2008, **24**, 469-478.
3. R. L. Rauck, *Pain Pract.*, 2009, **9**, 468-479.
4. B. H. McCarberg and R. L. Barkin, *Am. J. Ther.*, 2001, **8**, 181-186.
5. B. Mesgarpour, U. Griebler, A. Glechner, C. Kien, M. Strobelberger, M. Van Noord and A. Michalek-Sauberer, *Eur. J. Pain*, 2014, **18**, 605-616.
6. J. A. Gudin, *J. Pain Palliat. Care Pharmacother.*, 2013, **27**, 49-61.
7. P. Sloan and M. Davis, *J. Opioid Manag.*, 2014, **10**, 3.
8. K. Park, *J. Control. Release*, 2014, **190**, 3-8.
9. D. A. Miller, J. C. DiNunzio and R. O. Williams III, *Drug Dev. Ind. Pharm.*, 2008, **34**, 117-133.
10. A. Jacox, D. B. Carr and R. Payne, *N. Engl. J. Med.*, 1994, **330**, 651-655.
11. C. M. Amabile and B. J. Bowman, *Ann. Pharmacother.*, 2006, **40**, 1327-1335.
12. P. Storey, H. H. Hill, R. H. S. Louis and E. E. Tarver, *J. Pain Symptom Manage.*, 1990, **5**, 33-41.
13. S. Bajaj, A. Whiteman and B. Brandner, *Continuing Education in Anaesthesia, Critical Care & Pain*, 2011.
14. G. J. Lesser, S. A. Grossman, K. W. Leong, H. Lo and S. Eller, *Pain*, 1996, **65**, 265-272.
15. S. Grond, L. Radbruch and K. Lehmann, *Clin. Pharmacokinet.*, 2000, **38**, 59-89.
16. M. R. Prausnitz and R. Langer, *Nat. Biotech.*, 2008, **26**, 1261-1268.
17. T. R. Hoare and D. S. Kohane, *Polymer*, 2008, **49**, 1993-2007.
18. T. Vermonden, R. Censi and W. E. Hennink, *Chem. Rev.*, 2012, **112**, 2853-2888.
19. S. K. Gulrez, G. O. Phillips and S. Al-Assaf, *Hydrogels: methods of preparation, characterisation and applications*, INTECH Open Access Publisher, 2011.
20. M. Guvendiren, H. D. Lu and J. A. Burdick, *Soft Matter*, 2012, **8**, 260-272.
21. A. Dasgupta, J. H. Mondal and D. Das, *Rsc Adv.*, 2013, **3**, 9117-9149.

22. E. K. Johnson, D. J. Adams and P. J. Cameron, *J. Mater. Chem.*, 2011, **21**, 2024-2027.
23. C. Tomasini and N. Castellucci, *Chem. Soc. Rev.*, 2013, **42**, 156-172.
24. N. R. Lee, C. J. Bowerman and B. L. Nilsson, *Biomacromolecules*, 2013, **14**, 3267-3277.
25. M. Bibian, J. Mangelschots, J. Gardiner, L. Waddington, M. M. D. Acevedo, B. G. De Geest, B. Van Mele, A. Madder, R. Hoogenboom and S. Ballet, *J. Mater. Chem. B.*, 2015, **3**, 759-765.
26. O. D. Monera, T. J. Sereda, N. E. Zhou, C. M. Kay and R. S. Hodges, *J. Pept. Sci.*, 1995, **1**, 319-329.
27. F. Chambon and H. H. Winter, *J. Rheol.*, 1987, **31**, 683-697.
28. H. Winter, in *Permanent and Transient Networks*, Springer, 1987, pp. 104-110.
29. D. R. Picout and S. B. Ross-Murphy, *Scientific World J.*, 2003, **3**, 105-121.
30. R. K. Portenoy, A. Sciberras, L. Eliot, G. Loewen, J. Butler and J. Devane, *J. Pain Symptom Manage.*, 2002, **23**, 292-300.
31. C. Cloutier, J. Taliano, W. O'Mahony, M. Csanadi, G. Cohen, I. Sutton, D. Sinclair, M. Awde, S. Henein and L. Robinson, *Pain Res. Manag.*, 2013, **18**, 75.
32. X. Huang and C. S. Brazel, *J. Control. Release*, 2001, **73**, 121-136.
33. T. Holm, H. Räägel, S. E. Andaloussi, M. Hein, M. Mäe, M. Pooga and Ü. Langel, *Biochimica et Biophysica Acta (BBA)-Biomembranes*, 2011, **1808**, 1544-1551.
34. W. Chan and P. White, *Fmoc Solid Phase Peptide Synthesis a Practical Approach*, Oxford University Press: Oxford, 2000.
35. A. Novoa, S. Van Dorpe, E. Wynendaele, M. Spetea, N. Bracke, S. Stalmans, C. Betti, N. N. Chung, C. Lemieux, J. Zuegg, M. A. Cooper, D. Tourwé, B. De Spiegeleer, P. W. Schiller and S. Ballet, *J. Med. Chem.*, 2012, **55**, 9549-9561.

